JOURNAL OF BACTERIOLOGY, Oct. 1998, p. 5448–5453 Vol. 180, No. 20
0021-9193/98/$04.00+0

The 20S Proteasome of *Streptomyces coelicolor*

ISTVÁN NAGY,[1,2] TOMOHIRO TAMURA,[2] JOS VANDERLEYDEN,[1] WOLFGANG BAUMEISTER,[2] AND RENÉ DE MOT[1]*

F. A. Janssens Laboratory of Genetics, Catholic University of Leuven, B-3001 Heverlee, Belgium,[1] and Max-Planck-Institut für Biochemie, D-82152 Martinsried, Germany[2]

Received 20 July 1998/Accepted 13 August 1998

20S proteasomes were purified from *Streptomyces coelicolor* A3(2) and shown to be built from one α-type subunit (PrcA) and one β-type subunit (PrcB). The enzyme displayed chymotrypsin-like activity on synthetic substrates and was sensitive to peptide aldehyde and peptide vinyl sulfone inhibitors and to the *Streptomyces* metabolite lactacystin. Characterization of the structural genes revealed an operon-like gene organization (*prcBA*) similar to *Rhodococcus* and *Mycobacterium* spp. and showed that the β subunit is encoded with a 53-amino-acid propeptide which is removed during proteasome assembly. The upstream DNA region contains the conserved *orf7* and an AAA ATPase gene (*arc*).

Bacterial intracellular proteases have a variety of functions, including processing of precursor forms (such as removal of signal peptides in exported proteins), degradation of aberrant or damaged proteins (resulting from mutations or environmental stress), and inactivation of proteins that play key roles in regulatory processes. Such a diversity of tasks implicates the involvement of a complex set of proteolytic enzymes, as exemplified by the well-characterized *Escherichia coli* system (12). Some of these proteases, like Lon, have homologues in *Archaea* and *Eucarya*, whereas others seem to have a restricted interdomain distribution. Proteasomes were thought to be absent from *Bacteria*, until 20S proteasomes were discovered in the actinomycete *Rhodococcus* (42).

In eukaryotic cells, the 20S proteasome constitutes the proteolytic core of the 26S proteasome, which contains several accessory proteins (including ATPases) that enable selective proteolysis of ubiquitin-tagged substrates (9, 43), but such a 20S proteasome-associated regulatory entity has not yet been identified in *Bacteria* or *Archaea*. The 20S proteasome belongs to the group of self-compartmentalizing proteases, in which the active sites are confined to an interior compartment, created by self-assembly of a number of subunits (4, 21). The barrel-like structure of the 20S proteasome results from the stacking of four seven-membered rings: the two outer rings are composed of α-type subunits and the two inner rings are built from β-type subunits, in which the active sites are generated by autocatalytic processing during proteasome assembly. In eukaryotes such as yeast, different α-type and β-type subunits (seven of each) generate the 20S complex (14). In archaebacteria such as *Thermoplasma acidophilum*, the composition with only one α- and one β-type subunit is of minimal complexity (20), which has facilitated elucidation of the novel catalytic mechanism involving the N-terminal threonine of the β subunit generated upon autocatalytic maturation (37, 38). An intermediate degree of complexity is provided by the 20S proteasome of *Rhodococcus erythropolis* NI86/21, which is built from two different α- and β-type subunits (42, 49). The disclosure of proteasome-like genes by genomic sequencing of the related nocardioform actinomycetes *Mycobacterium leprae* and *Mycobacterium tuberculosis* (8, 22) and the subsequent characterization of the 20S proteasome genes in *Mycobacterium smegmatis* (18) revealed that the $\alpha_{14}\beta_{14}$ subunit composition, as found in archaebacteria, also occurs in eubacteria. In this communication, we report the biochemical and genetic characterization of the 20S proteasome from a phylogenetically distant actinomycete, *Streptomyces coelicolor* strain A3(2).

Purification of 20S proteasomes from *S. coelicolor*. *S. coelicolor* A3(2) was grown at 30°C for 3 days in medium containing casein (10 g/liter), yeast extract (5 g/liter), glucose (5 g/liter), glycine (5 g/liter), and 5 mM $MgCl_2$. Cells harvested from 3 liters of culture were washed with 50 mM HEPES buffer (pH 8.0) and resuspended in 100 ml of this buffer containing lysozyme (1 mg/ml). The cell suspension was kept on ice for 2 h. All further steps were carried out at 4°C, unless specified otherwise. DNase I (200 U) was added to the lysate, which was cleared by centrifugation at 61,700 × *g* for 1 h. Twenty milliliters of supernatant (containing about 230 mg of protein) was loaded on a Sepharose 6B column (3.2 by 86 cm; Pharmacia) and eluted with 50 mM Tris-HCl buffer (pH 7.5) containing 1 mM dithiothreitol (DTT) and 20% (vol/vol) glycerol (buffer A) at a flow rate of 46 ml/h. Fractions (5 ml) were collected and assayed for proteinase activity by using the synthetic substrate succinyl-Leu-Leu-Val-Tyr-7-amido-4-methylcoumarin (Suc-LLVY-AMC) (Bachem). The fluorigenic synthetic peptide (10 nmol) was incubated for 15 to 60 min at 37°C in 50 mM Tris-HCl buffer (pH 8.0) with the enzyme samples in a total reaction volume of 100 μl. The reaction was stopped by adding 100 μl of 10% (wt/vol) sodium dodecyl sulfate (SDS), and the fluorescence was measured to estimate the release of the 7-amido-4-methylcoumarin moiety. The active, high-molecular-mass fractions from three Sepharose 6B runs were pooled and loaded on a DEAE-Sephacel column (2.2 by 10 cm; Pharmacia) equilibrated with buffer A. Bound proteins were eluted with a 0 to 0.5 M NaCl linear gradient in 400 ml of buffer A. Fractions of 4 ml were collected. The fractions with proteolytic activity eluting at approximately 300 mM NaCl were pooled and dialyzed against 10 mM potassium phosphate buffer (pH 7.0) containing 1 mM DTT and 20% glycerol. The dialyzed sample was applied to a hydroxyapatite column (1.4 by 6 cm; Bio-Rad) equilibrated with 10 mM potassium phosphate buffer containing 20% (vol/vol) glycerol. A 10 to 300 mM potassium phos-

* Corresponding author. Mailing address: F. A. Janssens Laboratory of Genetics, Kardinaal Mercierlaan 92, B-3001 Heverlee, Belgium. Phone: 32 16 32 96 81. Fax: 32 16 32 19 66. E-mail: rene.demot@agr.kuleuven.ac.be.

TABLE 1. Purification of 20S proteasomes from *S. coelicolor*

Purification step	Total protein (mg)	Total activity (nmol h^{-1})	Sp act (nmol h^{-1} mg^{-1})	Purification factor	Yield (%)
Crude extract	700	3,200	4.6	1	100
Sepharose 6B	76.7	3,080	40.2	9	96
DEAE-Sephacel	13.7	2,160	158	34	68
Hydroxyapatite	3.37	1,683	499	109	53
Q Sepharose	0.26	1,333	5,127	1,115	42
Mono Q	0.057	880	15,439	3,356	28

phate linear gradient (100 ml) was used for elution, and 1.5-ml fractions were collected. Fractions (1.5 ml) with proteolytic activity on Suc-LLVY-AMC and which eluted at approximately 85 mM potassium phosphate were pooled and dialyzed against 25 mM Tris-HCl (pH 7.5) containing 1 mM DTT and 20% glycerol (buffer B). This sample was further purified on a Q Sepharose column (1.2 by 6 cm; Pharmacia). Fractions of 1 ml were collected during linear gradient elution with 200 to 600 mM NaCl (50 ml). Fractions (1 ml) with proteolytic activity, eluted at about 470 mM NaCl, were again pooled and dialyzed against buffer B. The final purification step involved linear gradient elution (0 to 0.6 M NaCl in 40 ml) from a Mono Q column. The fractions with proteasomes, eluted at approximately 480 mM NaCl, were dialyzed against buffer A and used for further characterization. Table 1 presents an overview of the purification procedure.

Characterization of the *S. coelicolor* 20S proteasome. Electron micrographs of negatively stained proteasomes show the two characteristic views (end-on and side-on) of the barrel-like 20S proteasome (Fig. 1). SDS-polyacrylamide gel electrophoresis analysis showed that the 20S proteasome preparation was homogeneous, revealing two bands of equal intensities with estimated relative molecular weights of 24,400 (β subunit) and 29,700 (α subunit) (Fig. 2). Purification of 20S proteasomes from the archaea *Methanosarcina thermophila* (24) and *Pyrococcus furiosus* (2), together with analyses of complete archaeal genomes (*Archaeoglobus fulgidus*, *Methanobacterium thermoautotrophicum*, and *Methanococcus jannaschii* [overview at http://www.tigr.org/tigr_home/tdb/mdb/mdb.html]), indicate that most archaeal 20S proteasomes have an $\alpha_{14}\beta_{14}$ subunit composition. However, we noted that the ongoing genomic sequencing of *Pyrococcus horikoshii* has already disclosed two distinct β-type subunit genes. The increased level of subunit complexity reported for the *R. erythropolis* NI86/21 20S proteasome (42, 49) has not been observed for 20S proteasomes from other eubacteria (actinomycetes), namely *Mycobacterium* spp. (8, 18) and *S. coelicolor* (this work).

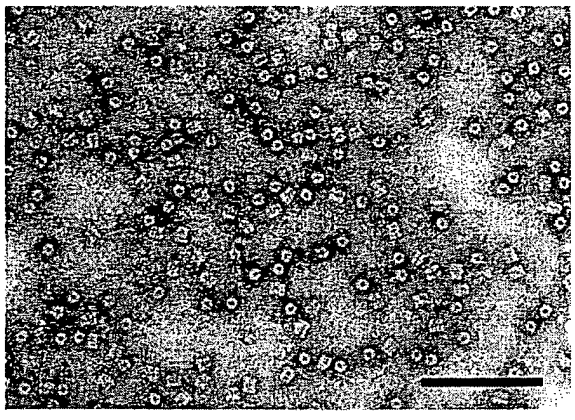

FIG. 1. Electron micrograph of 20S proteasomes from *S. coelicolor*, negatively stained with uranyl acetate (3), showing ring-shaped end-on views representing projections along the cylinder axis and rectangular side views corresponding to projections perpendicular to the cylinder axis. Bar, 100 nm.

FIG. 2. Tricine-SDS-polyacrylamide gel electrophoresis analysis of 2.28 μg of purified *S. coelicolor* 20S proteasomes (right lane). The sizes of the marker proteins (left lane) are 97.4, 66.2, 45.0, 31.0, 21.5, and 14.4 kDa (from top to bottom). The proteins were stained with Coomassie brilliant blue.

The substrate specificity of the *Streptomyces* 20S proteasome was determined at 37°C with various synthetic substrates (Bachem). The highest activity was obtained with Suc-LLVY-AMC (15.4 μmol h^{-1} mg^{-1} = 100%). Substantially lower activities were measured with two other chymotryptic substrates, benzoyloxycarbonyl-Gly-Gly-Leu-7-amido-4-methylcoumarin (0.78 μmol h^{-1} mg^{-1} = 5%) and succinyl-Ala-Ala-Phe-7-amido-4-methylcoumarin (0.15 μmol h^{-1} mg^{-1} = 1%), but no such activity was detectable with succinyl-Leu-Tyr-7-amido-4-methylcoumarin. Trypsin-like activity was assayed with benzoyloxycarbonyl-Gly-Gly-Arg-7-amido-4-methylcoumarin, *tert*-butyloxycarbonyl-Leu-Arg-Arg-7-amido-4-methylcoumarin, benzoyloxycarbonyl-Ala-Arg-Arg-7-amido-4-methylcoumarin, and benzoyl-Val-Gly-Arg-7-amido-4-methylcoumarin, whereas benzoyloxycarbonyl-Leu-Leu-Glu-β-naphthylamide (Z-LLE-βNA) was used as a peptidyl-glutamyl peptidase substrate; however, neither of these hydrolytic activities were demonstrated for the 20S proteasome from *Streptomyces*. This substrate spectrum is quite similar to that reported for the 20S proteasome from *Rhodococcus*, with high activity on chymotryptic substrates but no other detectable peptidase activities (42). High chymotrypsin-like activity is also a feature of the proteasomes from *T. acidophilum* (1, 10) and *P. furiosus* (2). Remarkably, the *M. thermophila* proteasome displays about 40% higher activity on Z-LLE-βNA than on Suc-LLVY-AMC (23).

The effects of some known proteasome inhibitors on the activity of the *Streptomyces* proteasome were determined (Fig. 3). Lactacystin (Affiniti) was a more potent inhibitor of the *Streptomyces* 20S proteasome than acetyl-Leu-Leu-norleucinal (Ac-LLnL) (Sigma) and benzoyloxycarbonyl-Leu-Leu-Leu-vinylsulfone (Z-LLL-VS). Very similar inhibition patterns were reported for the chymotrypsin-like activities of eukaryotic proteasomes preincubated with these inhibitors (6). For the *Thermoplasma* 20S proteasome, lactacystin is a moderately potent inhibitor (15% residual activity with 100 μM lactacystin [41]). Unlike Ac-LLnL, both lactacystin and Z-LLL-VS irreversibly inactivate proteasomes by covalent modification of the active-site threonine (6, 11, 25). Remarkably, lactacystin is produced by a *Streptomyces* strain (29). It will be of interest to investigate what may be the physiological implications for *Streptomyces*

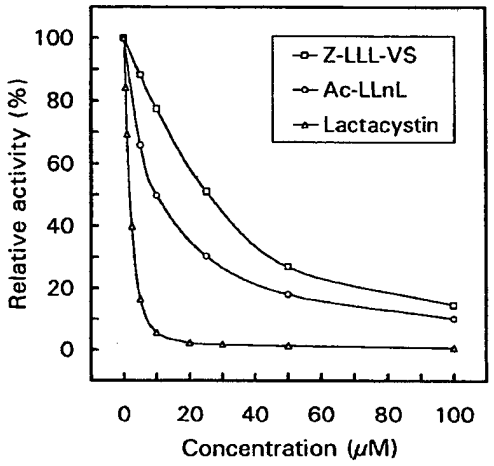

FIG. 3. Inhibition of the *S. coelicolor* 20S proteasome by Ac-LLnL, Z-LLL-VS, and lactacystin. Purified proteasome (0.912 μg) was incubated with inhibitor in 100 μl of Tris-HCl (pH 8.0) at room temperature for 1 h. Subsequently, 20 nmol of Suc-LLVY-AMC was added. After incubation at 37°C for 1 h, the reaction was stopped (by addition of 100 μl of 10% SDS) and the amount of 7-amido-4-methylcoumarin released was measured.

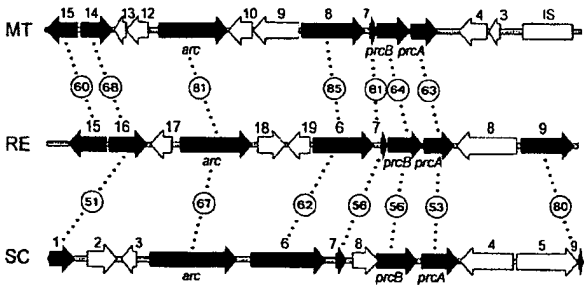

FIG. 4. Gene organization of the proteasome structural genes (*prcB*, *prcA*) and the flanking regions from *M. tuberculosis* (MT) (GenBank accession no. Z97559; 14,030 bp), *R. erythropolis* (RE) (GenBank accession no. U26422 and this work; 13,000 bp), and *S. coelicolor* (SC) (this work; 10,612 bp). The fragment shown for *Rhodococcus* represents the second proteasome operon. The ORFs in the respective DNA regions are numbered independently. For *M. tuberculosis*, the ORF numbering of cosmid MTCY261 is used. The box labeled IS represents one of the sixteen copies of IS*6110* present in the genome of *M. tuberculosis* H37Rv (8). Conserved ORFs and homologous genes are shown as filled arrows, and the extent of sequence conservation is indicated (numbers representing percentages of identical amino acids are circled).

cells that would produce both a major intracellular protease and a potent specific inhibitor of this enzyme. This is reminiscent of the regulation of activity of a trypsin-like protease that is essential for aerial mycelium formation by the autogenous inhibitor leupeptin (acetyl-leucine-leucine-arginal) and a leupeptin-inactivating enzyme in *Streptomyces exfoliatus* (17).

The optimum temperature for Suc-LLVY-AMC hydrolysis by the *Streptomyces* 20S proteasome was 55°C (data not shown), which is substantially lower than the temperature optima reported for *T. acidophilum* (85°C to 91°C [1, 10]), *P. furiosus* (95°C [2]), and *M. thermophila* (70°C to 75°C [23]). This difference probably reflects the thermophilic nature of these archaebacteria, as opposed to *Streptomyces* with an optimal growth temperature of about 30°C.

Cloning and characterization of the 20S proteasome structural genes from *S. coelicolor*. From *S. coelicolor* cells grown in glycine-containing medium and treated with lysozyme (1 mg/ml) at 30°C for 30 min, total DNA was isolated according to the method of Nagy et al. (26). A digoxigenin-labeled 960-bp *Sac*I-*Eco*RI fragment from the *R. erythropolis* $prcB_2A_2$ operon (42) was used as a probe for Southern hybridization (hybridization temperature, 60°C; washing was performed at 60°C with 7.5 mM sodium citrate containing 75 mM NaCl and 0.1% SDS) with total *S. coelicolor* DNA restricted by several endonucleases. Two hybridizing fragments (5.1-kb *Kpn*I and 8.0-kb *Sph*I fragments), covering a 10.6-kb region with the proteasome genes and flanking DNA, were cloned in pUC18 (generating pFAJ2594 and pFAJ2609, respectively). These clones were selected by colony hybridization with the *Rhodococcus* DNA probe from size-fractionated sublibraries. Subcloned fragments were subjected to automated sequence analysis (A.L.F. sequencer; Pharmacia), and subsequences were assembled with the ASSEMGEL program of PCGENE (IntelliGenetics). Potential codon regions were identified with the GCWIND program (40), relying on codon usage bias in genomes with high G+C contents.

Two open reading frames (ORFs) (*prcB*, *prcA*) with high homology to known eubacterial proteasome genes and organized in a similar way were identified (Fig. 4). The N-terminal sequence determined for the smaller subunit of the purified 20S proteasome (TTIVAVTF) was identical to the deduced amino acid sequence of PrcB after removal of a 53-amino-acid propeptide, characteristic of β-type subunits (Fig. 5A). The calculated molecular mass of the mature PrcB protein (24,428 Da) is in excellent agreement with the estimated M_r of 24,400. The propeptides of eubacterial β subunits are considerably longer (up to 65 residues for $PrcB_1$ of *R. erythropolis*) than those of archaebacterial β subunits, which typically consist of fewer than 10 amino acids. Zühl et al. (48) demonstrated that the propeptides of the *Rhodococcus* proteasome β subunits play a crucial role: they support the initial folding of the β subunits and promote the maturation of the holoproteasomes, in which the N-terminal active-site residue, threonine, becomes available following autocatalytic release of the propeptides. Such a chaperone-like function has also been assigned to the propeptide of a eukaryotic β-type proteasome subunit (7). A comparison of the currently available eubacterial propeptide sequences (Fig. 5A), reveals that two residues (HG) preceding the processing site (G-T peptide bond) are strictly conserved, as well as several residues in the middle part of the propeptide, whereas little conservation is apparent in the remainder of the sequences. It is likely that the central box with the consensus sequence SSFX(D/E)(F/Y/L)LX_4PEXLP is important for the function of the eubacterial propeptide. Such a box is not obviously present in eukaryotic propeptides, although a number of them contain the SF or AF sequence. No N-terminal sequence was obtained for the larger subunit, indicating that the amino terminus was blocked, a general characteristic of α-type subunits (42). The estimated M_r of this subunit (29,700) is somewhat higher than the calculated molecular mass of 27,883 Da.

Organization of the proteasome genomic regions in actinomycetes. Although purification and biochemical characterization of 20S proteasomes is currently limited to *Rhodococcus* (42) and *Streptomyces* (this work), genomic sequencing of *M. tuberculosis* (8) and *M. leprae*, and subsequent genetic analysis with *M. smegmatis* (18), now enables a comparison of the proteasome regions of representative actinomycetes to be made. To extend the known DNA sequence of the upstream region of $prcB_2A_2$ of *R. erythropolis* NI86/21, the flanking sequences of

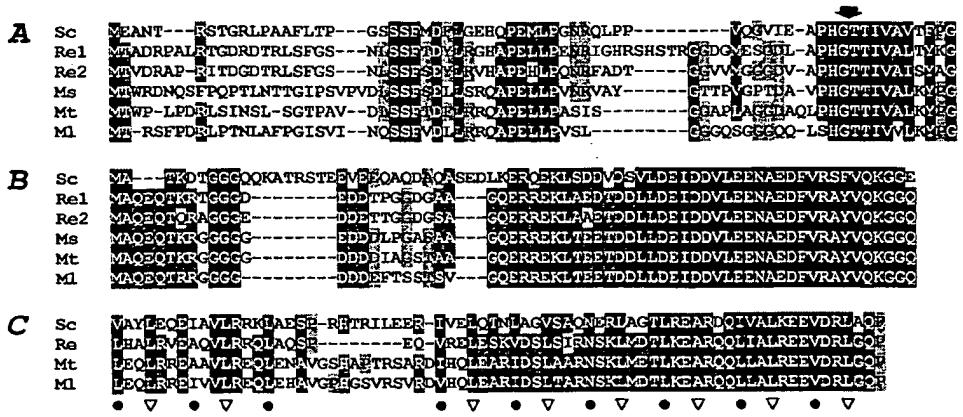

FIG. 5. Multiple sequence alignments of the proteasome β-subunit propeptides (A), the ORF7 sequences (B), and the N-terminal coiled-coil regions of ARC homologues (C) from the following actinomycetes: *M. leprae* (Ml), *M. smegmatis* (Ms), *M. tuberculosis* (Mt), *R. erythropolis* (Re1 and Re2, or Re), and *S. coelicolor* (Sc). Differential shading (three levels in panels A and B; two levels in panel C) reflects the degree of sequence conservation (identical or similar amino acids) at a given position. The propeptide cleavage sites are marked with an arrow, and the first 10 residues of the processed β subunits are shown in panel A. In panel C, the hydrophobic amino acids in positions 1 and 4 of the heptad repeats of the proposed coiled-coil structures of ARC proteins are labeled ● and ▽, respectively, and proline residues flanking coiled-coil segments are marked (in black on a shaded background).

the *arc* gene (46) were determined from the original λFAJ2029 clone (42).

Figure 4 reveals a patchy distribution of conserved genes and ORFs (apparently restricted to actinomycetes) with several interjacent ORFs that are not conserved between the different actinomycete species. The 20S proteasome structural genes of *S. coelicolor*, *prcB* and *prcA*, are separated by 61 bp. However, in *Rhodococcus* (42) and *Mycobacterium* (8, 18) spp., the *prcB* stop codon overlaps the *prcA* start codon, suggesting a translational coupling. The small conserved *orf7*, which overlaps the respective *prcB* genes in *Rhodococcus* and *Mycobacterium*, ends 580 bp upstream of the *Streptomyces prcB* gene. The *Streptomyces* ORF7 (72 amino acids) is somewhat larger than its counterparts from *Rhodococcus* and *Mycobacterium* (63 to 64 amino acids) but is quite similar, particularly in the C-terminal half, which contains a high proportion of acidic residues (Fig. 5B). The calculated pI value for *Streptomyces* ORF7 (3.7) and those of its homologues (3.6 to 3.7) are very similar. At present, it is not known whether this conserved ORF7 may exert a proteasome-related function. A possible ORF (*orf8*) is present between *orf7* and *prcB* and partially overlaps the latter, but no homologues were identified via database searches. Using a proteasome-specific probe, the proteasome genes have been mapped to the *Ase*I-I fragment (cosmid I4) of the *S. coelicolor* genome (16, 32).

Other conserved ORFs in the upstream region of *S. coelicolor* are *orf6*, *arc*, and *orf1* (partially sequenced). The *arc* gene product of *R. erythropolis*, ARC (for AAA ATPase forming ring-shaped complexes), was recently characterized (46). The linkage with proteasome genes and striking similarities in domain topology with those AAA-type ATPases forming part of the eukaryotic 26S proteasomes (5, 30) suggest a proteasome-related function for ARC, but this remains to be proven. A feature of the *Rhodococcus* ARC (and of the putative mycobacterial homologues) which it shares with proteasomal ATPases (33) is the presence of a potential N-terminal coiled-coil structure (46). By using the COILS server (http://www.isrec.isb-sib.ch/software/COILS_form.html), such an N-terminal segment was also predicted for *Streptomyces* ARC (Fig. 5C).

Unlike the gene organization in *Mycobacterium* and *Rhodococcus*, no ORFs are positioned between *arc* and another conserved (actinomycete-specific) ORF, *orf6*, in *Streptomyces* (Fig. 4). It is notable that the deduced ORF6 sequence has significant homology (about 40% identity) to the putative *orf9* product (27). A close homologue of ORF9 (partially sequenced) appears to be present in *S. coelicolor* as well (Fig. 4). In *M. tuberculosis*, but not in *M. leprae* (27), the equivalent of *orf9* is located in another part of the genome (cosmid MTCY49 [GenBank accession no. Z73966]). The presence of a copy of the promiscuous insertion sequence IS*6110* downstream of the proteasome genes in *M. tuberculosis* (Fig. 4) suggests that a genomic rearrangement may have taken place.

The *Streptomyces orf1* and its homologues in *Rhodococcus* (*orf16*) and *Mycobacterium* (*orf14*) encode putative methyltransferases with significant homologies to putative gene products from several archaebacteria (up to 37% identity for *P. horikoshii* [GenBank accession no. AB009528]). Collectively, these ORFs are distantly related to L-isoaspartyl protein carboxyl methyltransferases from various organisms; these are involved in the repair of L-isoaspartyl residues present in damaged proteins (45). For the remaining, nonconserved *Streptomyces* ORFs, homology searches revealed similarity to ferredoxins for ORF3, to LacI-related repressors (including *S. coelicolor* MalR [44]) for ORF4, and to transmembrane transporter proteins for ORF5, but the extent of the homology (<40% identity) did not allow reliable predictions of their possible functions.

Conclusions. The presence of 20S proteasomes in *Rhodococcus*, *Mycobacterium*, and *Streptomyces* spp. suggests that this cytoplasmic protease is widespread among actinomycetes (gram-positive bacteria with high G+C contents). The presence of proteasome-like genes in other representative actinomycete species (*Amycolatopsis methanolica*, *Brevibacterium linens*, *Clavibacter michiganense*, and *Corynebacterium glutamicum*) was confirmed by Southern hybridization with a rhodococcal proteasome gene probe (28). Furthermore, a polyclonal antibody raised against *Rhodococcus* proteasomes and cross-reacting with the *S. coelicolor* β-type subunit revealed the presence of putative β-type subunits in the SDS-insensitive, Suc-LLVY-AMC-active fractions obtained by glycerol gradient centrifugation of cell extracts from these species (28). Recently, proteasome genes have also been identified in *Frankia* sp. strain ACN 14a/ts-r (31).

Genomic sequencing data support the notion that 20S proteasome genes are confined to actinomycetes. In many other bacteria, including gram-positive bacteria (such as *Bacillus* spp.), a structurally different self-compartmentalizing protease, HslVU, is present (19, 34). This protease is built from the Clp-related ATPase subunit HslU (13, 39) and from the proteolytic HslV subunit, which shows some sequence homology (22) and similarity in catalytic mechanism (6, 47) to β-type proteasome subunits. In *E. coli*, a synergistic action of HslVU with other ATP-dependent proteases (such as Lon) in controlling the turnover of σ^{32} (sigma factor directing transcription of heat shock genes) and abnormal proteins has been observed (15). Lon homologues have been identified in mitochondria, archaebacteria, and eubacteria, including the fast-growing, nonpathogenic *M. smegmatis* (35). To our surprise, we were unable to identify a gene for a Lon homologue in the genome of the slow-growing *M. tuberculosis* H37Rv (8). It will be of interest to see whether this may also be the case for other pathogenic mycobacterial species, such as *M. leprae*.

Recently, it was shown that specific inhibition of proteasomes with Z-LLL-VS severely affected cell viability of the archaeon *T. acidophilum* following exposure to heat shock (36). However, an *M. smegmatis* mutant lacking proteasomes showed no obvious phenotypic alterations (18), indicating that an efficient backup system may exist in actinomycetes. The elucidation of the in vivo function of 20S proteasomes in actinomycetes should benefit from the identification of this protease and its structural genes in *Streptomyces*, since molecular genetic tools are much more advanced for this genus than for other actinomycetes.

Nucleotide sequence accession numbers. The nucleotide sequences of the *S. coelicolor* proteasome genes (including flanking DNA) and the nucleotide sequence of the *arc*-containing DNA region upstream of the *R. erythropolis* $prcB_2A_2$ genes have been deposited in the GenBank database under accession no. AF086832 and AF088800, respectively.

S. coelicolor A3(2) and *Amycolatopsis methanolica* NCIB 11946 were provided by J. Dusart (University of Liège, Liège, Belgium) and L. Dijkhuizen (University of Groningen, Groningen, The Netherlands), respectively. Mapping of the proteasome genes was carried out by H. Kieser and D. Hopwood (John Innes Centre, Norwich, United Kingdom). We are indebted to M. Bogyo (Harvard Medical School, Boston, Mass.) for providing the proteasome inhibitor Z-LLL-VS. M.-N. Pouch (Max Planck Institute of Biochemistry, Martinsried, Germany) kindly communicated results prior to publication and provided the bacterial proteasome antibodies. The GCWIND program was obtained from D. Shields (Trinity College, Dublin, Ireland).

These studies were supported by a grant from the Fund for Scientific Research—Flanders (Belgium) to R.D.M., a Senior Research Associate with this fund. Support from the Human Frontier Science Program to W.B. is gratefully acknowledged.

REFERENCES

1. **Akopian, T. N., A. F. Kisselev, and A. L. Goldberg.** 1997. Processive degradation of proteins and other catalytic properties of the proteasome from *Thermoplasma acidophilum*. J. Biol. Chem. **272**:1791–1798.
2. **Bauer, M. W., S. H. Bauer, and R. M. Kelly.** 1997. Purification and characterization of a proteasome from the hyperthermophilic archaeon *Pyrococcus furiosus*. Appl. Environ. Microbiol. **63**:1160–1164.
3. **Baumeister, W., B. Dahlmann, R. Hegerl, F. Kopp, L. Kuehn, and G. Pfeifer.** 1988. Electron microscopy and image analysis of the multicatalytic proteinase. FEBS Lett. **241**:239–245.
4. **Baumeister, W., J. Walz, F. Zühl, E. Seemüller.** 1998. The proteasome: paradigm of a self-compartmentalizing protease. Cell **92**:367–380.
5. **Beyer, A.** 1997. Sequence analysis of the AAA protein family. Protein Sci. **6**: 2043–2058.
6. **Bogyo, M., J. S. McMaster, M. Gaczynska, D. Tortorella, A. L. Goldberg, and H. Ploegh.** 1997. Covalent modification of the active site threonine of proteasomal β subunits and the *Escherichia coli* homolog HslV by a new class of inhibitors. Proc. Natl. Acad. Sci. USA **94**:6629–6634.
7. **Chen, P., and M. Hochstrasser.** 1996. Autocatalytic subunit processing couples active site formation in the 20S proteasome to completion of assembly. Cell **86**:961–972.
8. **Cole, S. T., R. Brosch, J. Parkhill, T. Garnier, C. Churcher, D. Harris, S. V. Gordon, K. Eiglmeier, S. Gas, C. E. Barry III, F. Tekaia, K. Badcock, D. Basham, D. Brown, T. Chillingworth, R. Connor, R. Davies, K. Devlin, T. Feltwell, S. Gentles, N. Hamlin, S. Holroyd, T. Hornsby, K. Jagels, A. Krogh, J. McLean, S. Moule, L. Murphy, K. Oliver, J. Osborne, M. A. Quail, M.-A. Rajandream, J. Rogers, S. Rutter, K. Seeger, J. Skelton, R. Squares, J. E. Sulston, K. Taylor, S. Whitehead, and B. G. Barrell.** 1998. Deciphering the biology of *Mycobacterium tuberculosis* from the complete genome sequence. Nature **393**:537–544.
9. **Coux, O., K. Tanaka, and A. Goldberg.** 1996. Structure and functions of the 20S and 26S proteasomes. Annu. Rev. Biochem. **65**:801–847.
10. **Dahlmann, B., L. Kuehn, A. Grziwa, P. Zwickl, and W. Baumeister.** 1992. Biochemical properties of the proteasome from *Thermoplasma acidophilum*. Eur. J. Biochem. **208**:789–797.
11. **Fenteany, G., R. F. Standaert, W. S. Lane, S. Choi, E. J. Corey, and S. L. Schreiber.** 1995. Inhibition of proteasome activities and subunit-specific amino-terminal threonine modification by lactacystin. Science **268**:726–731.
12. **Gottesman, S.** 1996. Proteases and their targets in *Escherichia coli*. Annu. Rev. Genet. **30**:456–506.
13. **Gottesman, S., M. R. Maurizi, and S. Wickner.** 1997. Regulatory subunits of energy-dependent ATPases. Cell **91**:435–438.
14. **Groll, M., L. Ditzel, J. Löwe, D. Stock, M. Bochtler, H. D. Bartunik, and R. Huber.** 1997. Structure of the 20S proteasome from yeast at 2.4 Å resolution. Nature **386**:463–471.
15. **Kanemori, M., K. Nishihara, H. Yanagi, and T. Yura.** 1997. Synergistic roles of HslVU and other ATP-dependent proteases in controlling in vivo turnover of σ^{32} and abnormal proteins in *Escherichia coli*. J. Bacteriol. **179**:7219–7225.
16. **Kieser, H., and D. Hopwood.** Personal communication.
17. **Kim, I. S., Y. B. Kim, and K. J. Lee.** 1998. Characterization of the leupeptin-inactivating enzyme from *Streptomyces exfoliatus* SMF13 which produces leupeptin. Biochem. J. **331**:539–545.
18. **Knipfer, N., and T. E. Shrader.** 1997. Inactivation of the 20S proteasome in *Mycobacterium smegmatis*. Mol. Microbiol. **25**:375–383.
19. **Larsen, C. N., and D. Finley.** 1997. Protein translocation channels in the proteasome and other proteases. Cell **91**:431–434.
20. **Löwe, J., D. Stock, B. Jap, P. Zwickl, W. Baumeister, and R. Huber.** 1995. Crystal structure of the 20S proteasome from the archaeon *T. acidophilum* at 3.4 Å resolution. Science **268**:533–539.
21. **Lupas, A., J. M. Flanagan, T. Tamura, and W. Baumeister.** 1997. Self-compartmentalizing proteases. Trends Biochem. Sci. **22**:399–404.
22. **Lupas, A., F. Zühl, T. Tamura, S. Wolf, I. Nagy, R. De Mot, and W. Baumeister.** 1997. Eubacterial proteasomes. Mol. Biol. Rep. **24**:125–131.
23. **Maupin-Furlow, J. A., H. C. Aldrich, and J. G. Ferry.** 1998. Biochemical characterization of the 20S proteasome from the methanoarchaeon *Methanosarcina thermophila*. J. Bacteriol. **180**:1480–1487.
24. **Maupin-Furlow, J. A., and J. G. Ferry.** 1995. A proteasome from the methanogenic archaeon *Methanosarcina thermophila*. J. Biol. Chem. **270**:28617–28622.
25. **McCormack, T., W. Baumeister, L. Grenier, C. Moomaw, L. Plamondon, B. Pramanik, C. Slaughter, F. Soucy, R. Stein, F. Zühl, and D. Lawrence.** 1997. Active site-directed inhibitors of *Rhodococcus* 20S proteasome. J. Biol. Chem. **272**:26103–26109.
26. **Nagy, I., G. Schoofs, F. Compernolle, P. Proost, J. Vanderleyden, and R. De Mot.** 1995. Degradation of the thiocarbamate herbicide EPTC (*S*-ethyl dipropylcarbamothioate) and biosafening by *Rhodococcus* sp. strain NI86/21 involve an inducible cytochrome P-450 system and aldehyde dehydrogenase. J. Bacteriol. **177**:676–687.
27. **Nagy, I., G. Schoofs, J. Vanderleyden, and R. De Mot.** 1997. Further sequence analysis of the DNA regions with the *Rhodococcus* 20S proteasome structural genes reveals extensive homology with *Mycobacterium leprae*. DNA Sequence **7**:225–228.
28. **Nagy, I., T. Tamura, W. Baumeister, and R. De Mot.** Unpublished data.
29. **Omura, S., T. Fujimoto, K. Otoguro, K. Matsuzaki, R. Moriguchi, H. Tanaka, and Y. Sasaki.** 1991. Lactacystin, a novel microbial metabolite, induces neuritogenesis of neuroblastoma cells. J. Antibiot. **44**:113–116.
30. **Patel, S., and M. Latterich.** 1998. The AAA team: related ATPases with diverse functions. Trends Cell Biol. **8**:65–71.
31. **Pouch, M.-N., and W. Baumeister.** Unpublished data.
32. **Redenbach, M., H. M. Kieser, D. Denapaite, A. Eichner, J. Cullum, H. Kinashi, and D. A. Hopwood.** 1996. A set of ordered cosmids and a detailed genetic and physical map for the 8 Mb *Streptomyces coelicolor* A3(2) chromosome. Mol. Microbiol. **21**:77–96.
33. **Richmond, C., C. Gorbea, and M. Rechsteiner.** 1997. Specific interactions between ATPase subunits of the 20S protease. J. Biol. Chem. **272**:13403–13411.
34. **Rohrwild, M., G. Pfeifer, U. Santarius, S. A. Müller, H.-C. Huang, A. Engel, W. Baumeister, and A. L. Goldberg.** 1997. The ATP-dependent HslVU pro-

tease from *Escherichia coli* is a four-ring structure resembling the proteasome. Nat. Struct. Biol. 4:133–139.
35. **Roudiak, S. G., A. Seth, N. Knipfer, and T. E. Shrader.** 1998. The Lon protease from *Mycobacterium smegmatis*: molecular cloning, sequence analysis, functional expression, and enzymatic characterization. Biochemistry 37: 377–386.
36. **Ruepp, A., C. Eckerskorn, M. Bogyo, and W. Baumeister.** 1998. Proteasome function is dispensable under normal but not under heat shock conditions in *Thermoplasma acidophilum*. FEBS Lett. 425:87–90.
37. **Seemüller, E., A. Lupas, and W. Baumeister.** 1996. Autocatalytic processing of the 20S proteasome. Nature 382:468–470.
38. **Seemüller, E., A. Lupas, D. Stock, J. Löwe, R. Huber, and W. Baumeister.** 1995. Proteasome from *Thermoplasma acidophilum*: a threonine protease. Science 268:579–582.
39. **Seol, H., S. J. Yoo, D. H. Shin, Y. K. Shim, M.-S. Kang, A. L. Goldberg, and C. H. Chung.** 1997. The heat-shock protein HslVU from *Escherichia coli* is a protein-activated ATPase as well as an ATP-dependent proteinase. Eur. J. Biochem. 247:1143–1150.
40. **Shields, D. C., D. G. Higgins, and P. M. Sharp.** 1992. GCWIND: a microcomputer program for identifying open reading frames according to codon positional G+C content. Comput. Appl. Biosci. 8:521–523.
41. **Tamura, T., and W. Baumeister.** Unpublished data.
42. **Tamura, T., I. Nagy, A. Lupas, F. Lottspeich, Z. Cejka, G. Schoofs, K. Tanaka, R. De Mot, and W. Baumeister.** 1995. The first characterization of a eubacterial proteasome: the 20S complex of *Rhodococcus*. Curr. Biol. 5: 766–774.
43. **Tanaka, K.** 1998. Proteasomes: structure and biology. J. Biochem. 123:195–204.
44. **van Wezel, G. P., J. White, P. Young, P. W. Postma, and M. J. Bibb.** 1997. Substrate induction and glucose repression of maltose utilization by *Streptomyces coelicolor* A3(2) is controlled by *malR*, a member of the *lacI-galR* family of regulatory genes. Mol. Microbiol. 23:537–549.
45. **Visick, J. E., and S. Clarke.** 1995. Repair, refold, recycle: how bacteria can deal with spontaneous and environmental damage to proteins. Mol. Microbiol. 16:835–845.
46. **Wolf, S., I. Nagy, A. Lupas, G. Pfeifer, Z. Cejka, S. A. Müller, A. Engel, R. De Mot, and W. Baumeister.** 1998. Characterization of ARC, a divergent member of the AAA ATPase family from *Rhodococcus erythropolis*. J. Mol. Biol. 277:13–25.
47. **Yoo, S. J., Y. K. Shim, I. S. Seong, J. H. Seol, M.-S. Kang, and C. H. Chung.** 1997. Mutagenesis of two N-terminal Thr and five Ser residues in HslV, the proteolytic component of the ATP-dependent HslVU protease. FEBS Lett. 412:57–60.
48. **Zühl, F., E. Seemüller, R. Golbik, and W. Baumeister.** 1997. Dissecting the assembly pathway of the 20S proteasome. FEBS Lett. 418:189–194.
49. **Zühl, F., T. Tamura, I. Dolenc, Z. Cejka, I. Nagy, R. De Mot, and W. Baumeister.** 1997. Subunit topology of the *Rhodococcus* proteasome. FEBS Lett. 400:83–90.